

# Electrochemical Impedance Analysis Applied to HEVs Energy Storage

by

Toshiyuki SAKAMOTO<sup>\*1</sup> and Yuhei YAMASHITA<sup>\*2</sup>

(Received on Mar. 30, 2013 and accepted on Jul. 11, 2013)

## Abstract

Nickel-metal hydride (Ni-MH) batteries are widely installed for traction energy storage in HEVs. A battery deteriorates due to chemical reactions. This study is an investigation of battery deterioration parameters and AC impedance characteristics. Battery SOC (State of charge) and battery temperature are major deterioration parameters. Experimental tests were done on the two deterioration parameters which set values widely considered to represent real world usages. The AC impedance of the battery was measured in stable conditions after each test. Battery AC impedance spectroscopy shows the shape of a Nyquist diagram on a complex plane and is able to verify the battery deterioration in both the parameters of the battery SOC and the battery temperature, in the two types of Ni-MH batteries, which are a super lattice structure and a nominal AB5 one.

**Keywords:** Automobile, Battery, Measurement, Impedance, Analysis

## 1. Introduction

A traction battery installed on Hybrid Electric Vehicles (HEVs), has a deterioration of life with chemical reactions. This study investigates a possibility extent that a battery AC impedance characteristic represents the battery deterioration level. A battery is focused on a Nickel-metal hydride (Ni-MH) battery which is used widely as traction energy storage in HEVs. Major battery deterioration parameters are enumerated a battery state of charge (SOC) which shows the battery charged amount, and a battery temperature<sup>1)</sup>. Battery deterioration level can be verified by a discharge capacity test and a high rate discharge test, which are both precise measurements on a laboratory scale condition. And another method, the battery deterioration level can be detected easily to measure the battery AC impedance on a laboratory scale condition<sup>2), 3)</sup>. The study final object is a verification of the battery AC impedance method which is applied to check a battery state of health (SOH) on an on-board battery under operating conditions.

In this first study we examined a relation between the battery AC impedance characteristics and the battery deterioration parameters. The examination test condition is

set on an estimated condition on a real world usage.

## 2. Experimental method

### 2.1 Battery

Experimental batteries are commercial model of Ni-MH secondary batteries in two types. One of which is the most popular AB5 alloy type and the other is a super lattice alloy type. Herewith, the AB5 alloy type assigns "A" type, and the super lattice alloy type assigns "B" type. "A" type battery specification is 1900mAh of rated capacity, EVOLTA (type; HHR-3MWS) manufactured by Panasonic Co., Ltd. "B" type battery specification is also 1900mAh of rated capacity, Eneloop (type; HR-3UTGB) manufactured by Panasonic Co., Ltd. The examination is carried out with the brand-new battery after activation under both charged and discharged cycles.

### 2.2 Theory

A battery impedance spectrum plots on a complex plane which is a notational system. The battery AC impedance has two parts which are a real part  $Z'$  on a horizontal axis and an imaginary part  $Z''$  on a vertical axis respectively. The plotted figure is generally called a Nyquist diagram. Fig. 1 shows battery chemical impedance on equivalent circuit elements

\*1 Professor, Department of Prime Mover Engineering

\*2 Graduate Student, Course of Mechanical Engineering

both with a resistor component  $R$  and with a condenser component  $C$ . Equation (1) shows the battery chemical impedance  $Z$  in Fig. 1<sup>4), 5)</sup>.

$$Z = R_{sol} + \frac{R_{ct}}{1 + j\omega R_{ct} C_{dl}} \quad (1)$$

Equation (1) consists of a real part  $Z'$  and an imaginary part  $Z''$  shown in Eq. (2).

$$Z = Z' - jZ'' \quad (2)$$

$$Z' = R_{sol} + \frac{R_{ct}}{1 + \omega^2 R_{ct}^2 C_{dl}^2} \quad (3)$$

$$Z'' = \frac{\omega R_{ct}^2 C_{dl}}{1 + \omega^2 R_{ct}^2 C_{dl}^2} \quad (4)$$

$$\left( Z' - R_{sol} - \frac{R_{ct}}{2} \right)^2 + Z''^2 = \left( \frac{R_{ct}}{2} \right)^2 \quad (5)$$

herewith

$R_{sol}$  : battery electrolyte resistance

$R_{ct}$  : charge transfer resistance

$C_{dl}$  : electric double layer resistance

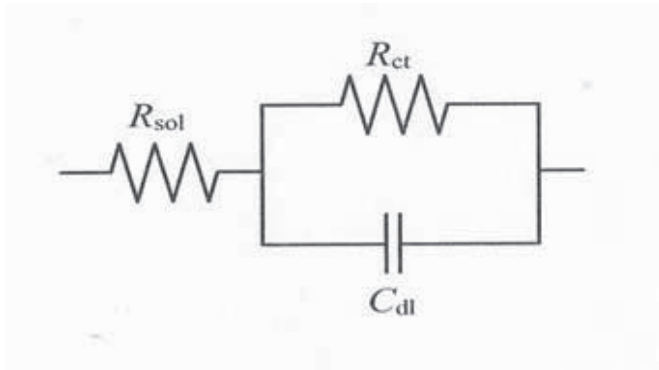


Fig. 1 Fundamental battery chemical impedance model with RC circuit components

### 2.3 Method

The experimental test condition is as follows; the battery SOC is set by a charge-discharge electrical load control unit (type; HJ-20) manufactured by Hokuto Denko Co., Ltd. The battery temperature is set in a thermostatic chamber (type; LU-113) manufactured by Espec Co., Ltd. The battery AC impedance spectroscopy with sweeping frequency is measured by a chemical impedance meter (type; 3532) manufactured by Hioki Co., Ltd. The measurement procedure

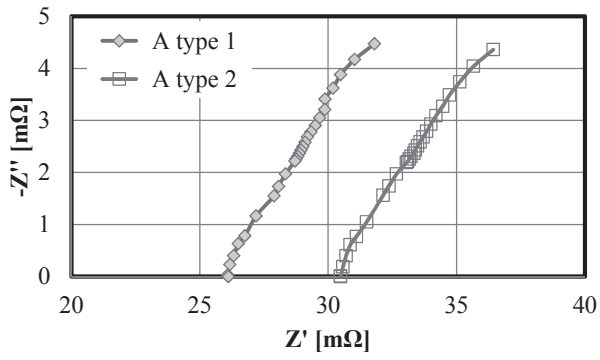
consists of four steps per cycle that is a charge step, a measurement step, a discharge step and a measurement step. The battery AC impedance measurement has done after the battery condition becomes steady level. The battery connected to a measurement wire harness where is attached to solder pieces of metal which prevents a voltage drop of the contact resistance<sup>6)</sup>. This is because the battery impedance is so small which level is a few milli-ohm, and necessary to reduce any ohmic loss during the battery AC impedance measurement. The battery AC impedance spectroscopy is measured at a different frequency to the battery. The AC impedance measurement is done on the frequency range from 4Hz to 20Hz in each 1Hz step, on the frequency range from 20Hz to 90Hz in each 10Hz step and on the frequency range from 100Hz to 1000Hz over in each 100Hz step. The results of the AC impedance measurement reveals both battery impedance components of the real part  $Z'$  and of the imaginary part  $Z''$ .

## 3. Experimental study

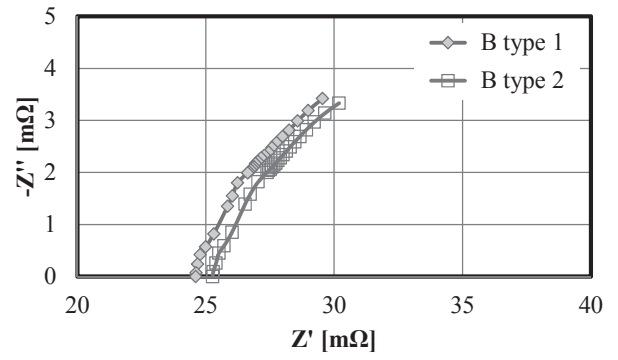
### 3.1 AC impedance spectroscopy of selected %SOC

Figure 2 shows AC impedance spectroscopy in an activation battery, the experimental battery of "A" type (A type 1 to A type 2). Fig. 2(a), Fig. 2(b), Fig. 2(c), and Fig. 2(d) show the battery capacity amount which is 100%, 75%, 50%, and 25% SOC respectively. In Fig. 2(a), two sets of "A" type battery AC impedance spectroscopy plots together in the graph. The spectroscopy curve which plots in the same figure traced on the graph. Even though the edge plots of AC impedance spectroscopy is in the different value of the real part  $Z'$  on the horizontal axis ( $Z''=0$ ). In Fig 2(b) to Fig. 2(d), two sets of "A" type battery AC impedance spectroscopy curve trace on the same figure in each graph. It can be said that the AC impedance spectroscopy curve trace like the same figure in each battery SOC but the curve figure is different in different battery SOC.

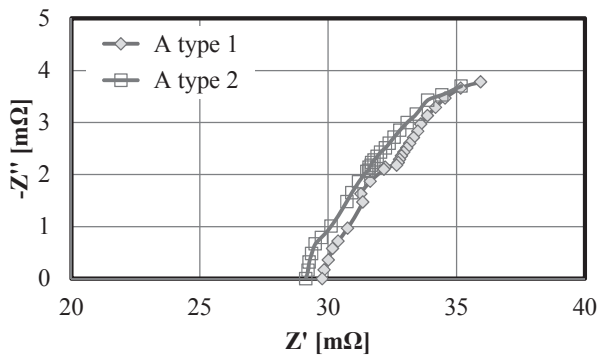
Figure 3 shows AC impedance spectroscopy in an activation battery, the experimental battery of "B" type (B type 1 to B type 2). Fig. 3(a), Fig. 3(b), Fig. 3(c), and Fig. 3(d) show the battery capacity amount which is 100%, 75%, 50%, and 25% SOC respectively. It can be said that AC impedance spectroscopy curve of "B" type battery which trace like the same figure at the same battery SOC but the figure is different in different battery SOC.



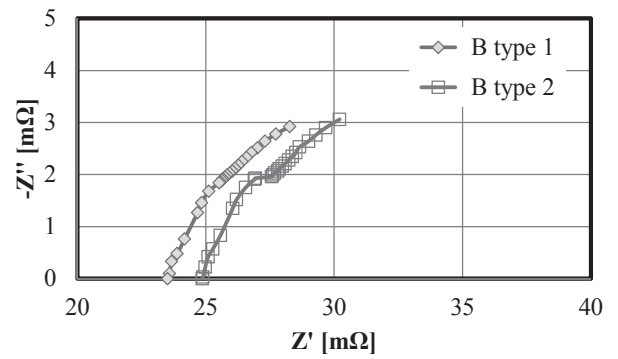
(a) 100% SOC



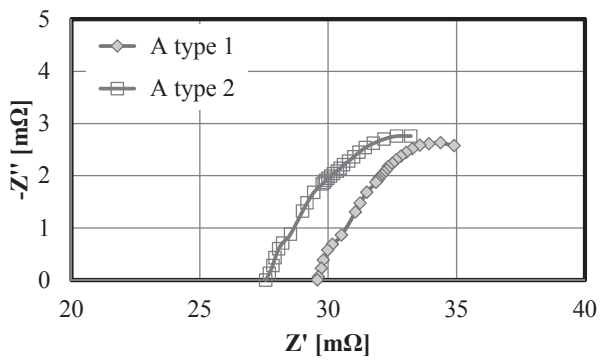
(a) 100% SOC



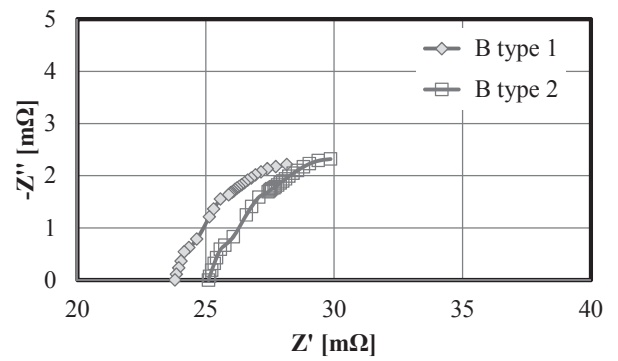
(b) 75% SOC



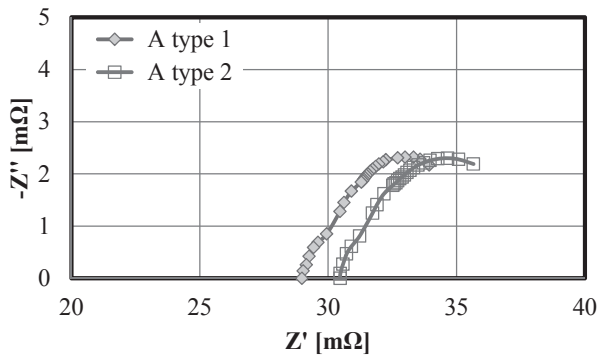
(b) 75% SOC



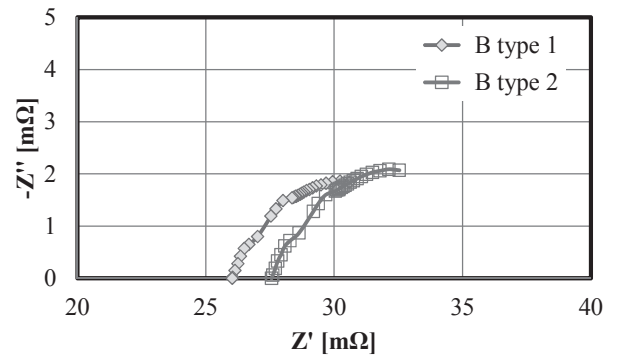
(c) 50% SOC



(c) 50% SOC



(d) 25% SOC

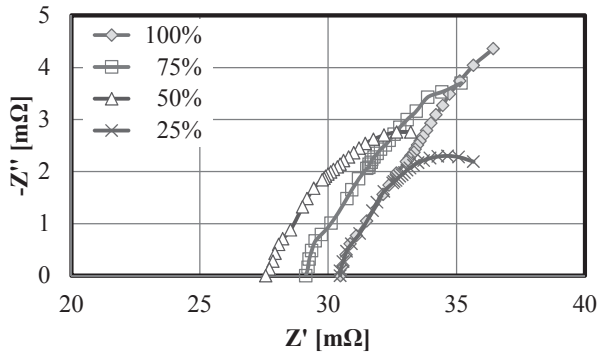


(d) 25% SOC

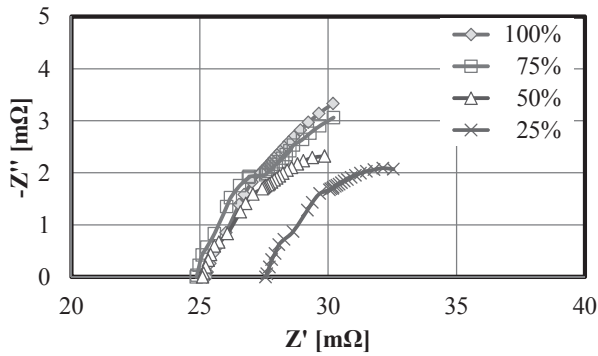
Fig. 2 AC impedance spectroscopy of A type battery (Selected %SOC, activation)

Fig. 3 AC impedance spectroscopy of B type battery (Selected %SOC, activation)

Figure 4 shows AC impedance of the activated batteries both “A” type (A type 2) and “B” type (B type 2) of the selected %SOC, 100%, 75%, 50%, and 25%. Fig. 4(a) shows “A” type (A type 2) battery of the selected %SOC. Fig. 4(b) shows “B” type (B type 2) battery of the selected %SOC. It can be observed that the radius of Nyquist diagram is large circle along with the battery SOC (i.e. the battery charged volume) in each type of battery.



(a) A type 2



(b) B type 2

Fig. 4 AC impedance spectroscopy (Selected %SOC, activation)

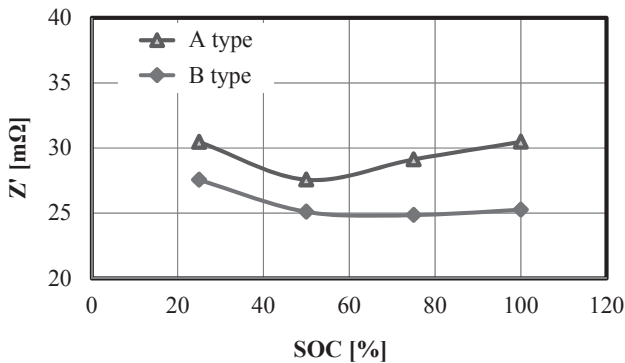


Fig. 5 AC impedance characteristic ( $Z''=0$ , activation)

It can be said that the real part  $Z'$  on the horizontal axis ( $Z''=0$ ) in Fig. 2 and in Fig. 3 which shall be represent the battery AC impedance. Fig. 5 shows AC impedance both of “A” type (A type 2) battery and of “B” type (B type 2) battery in the selected %SOC which are connected with a line in each type of battery. “A” type battery AC impedance is larger level than “B” type battery AC impedance in all of the selected %SOC. “A” type battery AC impedance has a bottom value in 50% SOC. “B” type battery has also a bottom value in 50% SOC and maintains the level over 50% SOC. Both battery types have the bottom AC impedances which mean both type batteries shall operate under the bottom SOC to realize low energy loses.

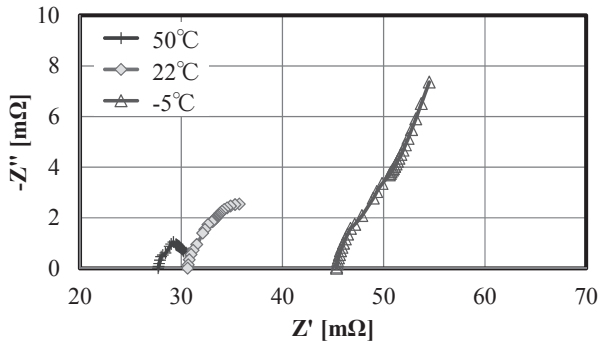
### 3.2 AC impedance spectroscopy of selected %SOC and battery temperature

Figure 6 shows AC impedance spectroscopy of the second experimental battery of “A” type (A type 2) which has been activated. The AC impedance spectroscopy plots in the selected %SOCs and of the selected battery temperatures.

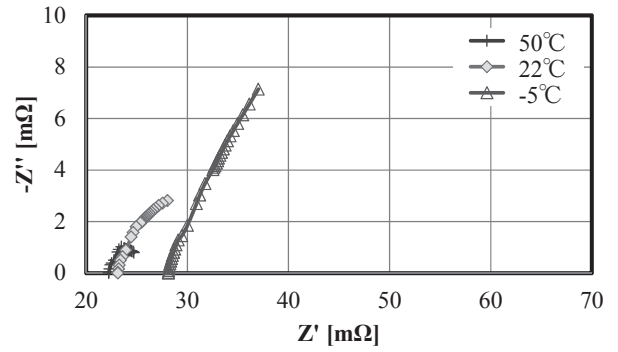
Concerning with the long life time of battery, Ni-MH battery temperature shall be controlled under the nominal ranges from 20 to 25 degrees C. In actual usage, on-board battery temperature is controlled under the allowable life time ranges from -5 to 45 degrees C. In this experiment, the battery temperature ranges are set in high level side which is 50 degrees C and in low level side which is -5 degrees C.

Fig. 6(a) shows AC impedance spectroscopy in 100% SOC. Fig. 6(a) plots AC impedance spectroscopy at three temperature conditions which are 50 degrees C, -5 degrees C and a standard temperature 22 degrees C for reference. Fig. 6(b), Fig. 6(c) and Fig. 6(d) show AC impedance spectroscopy in 75% SOC, in 50% SOC and in 25% SOC respectively. The high battery temperature has fallen AC impedance in lower level which can be seen both a real part  $Z'$  and an imaginary part  $Z''$ . The battery AC impedance in the low battery temperature has arisen to a high value shown in both a real part and an imaginary part.

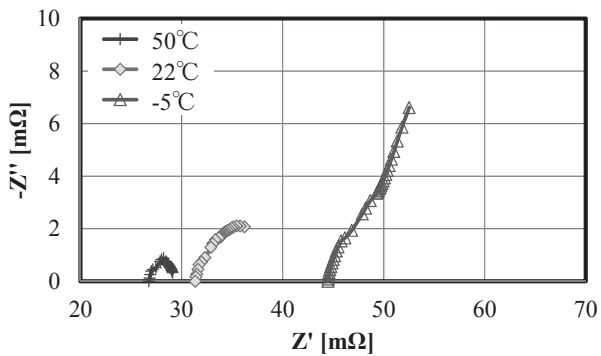
The battery temperature difference from the standard temperature 22 degrees C to the high level of 50 degrees C is the same degree from the standard temperature 22 degrees C to the low level of -5 degrees C. The battery AC impedance spectroscopies are much different. The battery AC impedance spectroscopy from the standard temperature 22 degrees C to -5 degrees C is notational value. This fact shows the battery characteristic is much down and hard to perform in the low temperature. Fig. 6(d) shows that the battery AC impedance is much rise and the battery performance is much down in both the low battery temperature (-5 degrees C) and the low battery SOC (25% SOC).



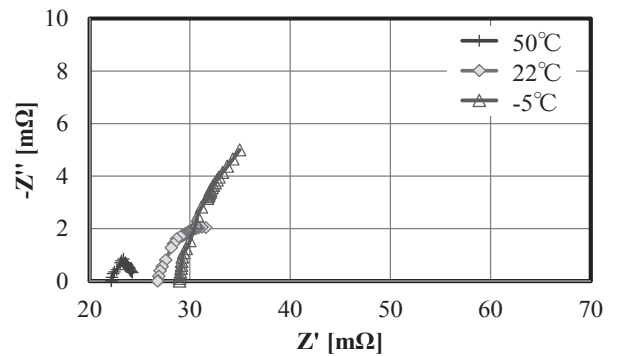
(a) A type 2 (100% SOC)



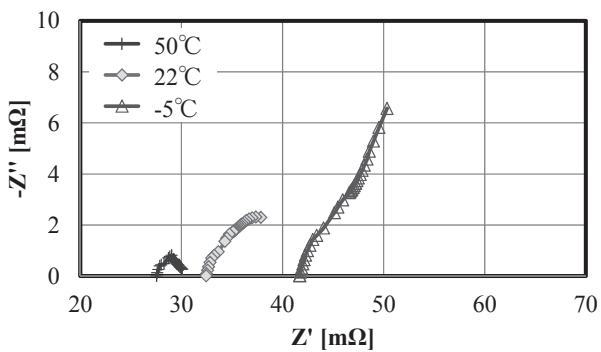
(a) B type 2 (100% SOC)



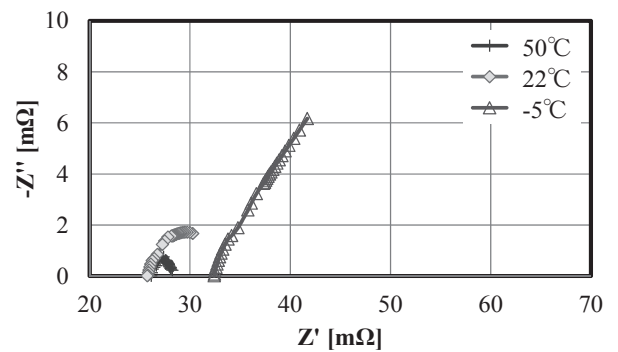
(b) A type 2 (75% SOC)



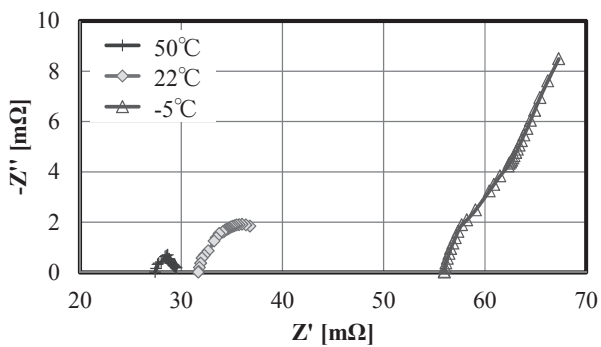
(b) B type 2 (75% SOC)



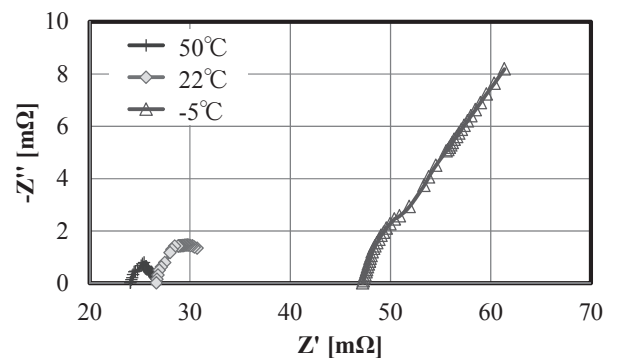
(c) A type 2 (50% SOC)



(c) B type 2 (50% SOC)



(d) A type 2 (25% SOC)



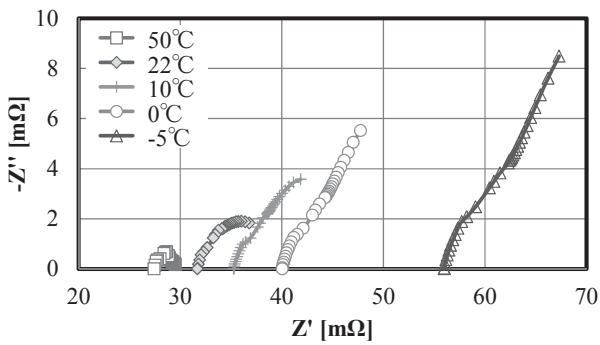
(d) B type 2 (25% SOC)

Fig. 6 AC impedance spectroscopy of A type battery (Selected %SOC, activation)

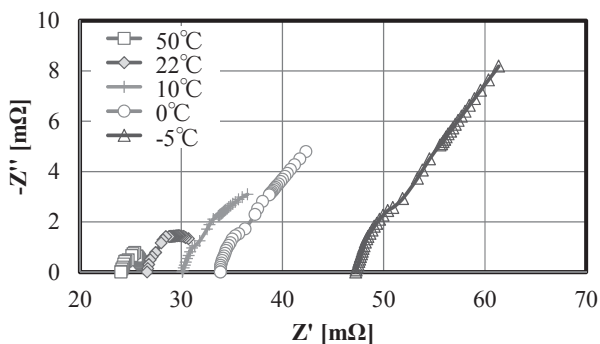
Fig. 7 AC impedance spectroscopy of B type battery (Selected %SOC, activation)

Figure 7 shows AC impedance spectroscopy of the second experimental battery of “B” type (B type 2) being activated. The AC impedance spectroscopy plots in the selected %SOCs and of selected battery temperatures. Fig. 7(a), Fig. 7(b), Fig. 7(c), and Fig. 7(d) show AC impedance spectroscopy in 100% SOC, in 75% SOC, in 50% SOC, and in 25% SOC respectively. The battery AC impedance are concentrated at a narrow range on the real part of the x-axis at  $Z''=0$  which shows in each selected battery temperature with an exceptional spectroscopy in both the low battery temperature (-5 degrees C) and the low battery SOC (25% SOC). AC impedance spectroscopy of “B” type (B type 2) being activated shows like the same of “A” type (A type 2) one as follows;

The battery AC impedance in the high level battery temperature has decreased the value in both the real part and the imaginary part. The battery AC impedance in the low level battery temperature has increased the value in both the real part and the imaginary part.



(a) A type 2



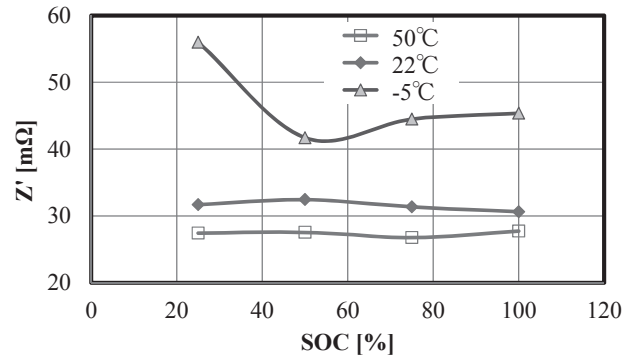
(b) B type 2

Fig. 8 AC impedance spectroscopy (25% SOC, activation)

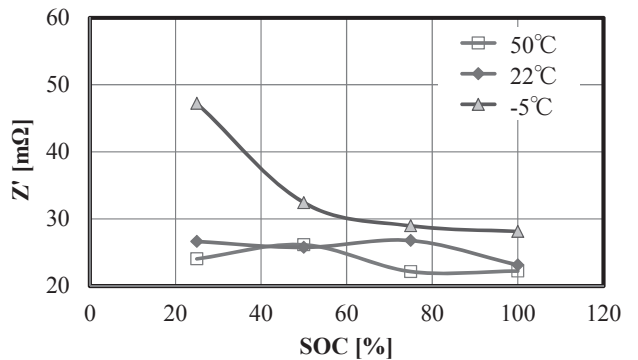
Figure 8 shows AC impedance spectroscopy of 25% SOC and of the selected battery temperatures which are 50, 22, 10, 0, and -5 degrees C. Fig. 8(a) shows AC impedance

spectroscopy of “A” type (A type 2) with activation. Fig. 8(b) shows AC impedance spectroscopy of “B” type (B type 2) with activation. Fig. 6 and Fig.7 show that the AC impedance spectroscopy of the battery temperature in low range is -5 degrees C alone. And there is the notational distance of AC impedance between the standard temperature 22 degrees C and -5 degrees C. Fig. 8 increase battery temperature plots 10 degrees C and 0 degrees C. But still exists a wide distance of AC impedance from 0 degrees C to -5 degrees C which can be seen both type of batteries. The battery performance is notational down below minus battery temperature owing to a poor chemical reaction even though in the different battery alloy structure.

Figure 9 shows AC impedance of the activated batteries both “A” type (A type 2) and “B” type (B type 2) of the selected battery temperatures which are 50 degrees C, 22 degrees C, and -5 degrees C. AC impedance in each selected %SOC which are connected with a line in each battery temperature and in each type of battery.



(a) A type 2



(b) B type 2

Fig. 9 AC impedance spectroscopy ( $Z''=0$ , activation)

“A” type battery AC impedance is larger level than “B” type battery in each battery temperature. Fig. 9(a) shows AC impedance spectroscopy of “A” type (A type 2) with

activation. In all of the selected %SOC, the lower degree of the battery temperature makes the battery AC impedance rise. Fig. 9(b) shows AC impedance spectroscopy of “B” type (B type 2) with activation. In all of the selected %SOC, the lowest degree of the battery temperature (-5 degrees C) in 25% SOC is obviously a high value of battery AC impedance. But over 50% SOC, the battery AC impedances get close each other in all of the selected battery temperature. In addition to that the battery temperatures of the standard (22 degrees C) and of the high level (50 degrees C) are closed lines

#### 4. Conclusion

This study verified with two types of different alloy structure of Ni-MH battery and acquired following knowledge.

- (1) The super lattice structure alloy type battery (B type) shows lower AC impedance than the nominal AB5 alloy type battery (A type).
- (2) Both battery types have the bottom AC impedances in 50% SOC (A type) and over (B type). The bottom SOC battery control may realize low energy losses.
- (3) Both battery types prominently increase the AC impedance in the low battery temperature (-5 degrees C) under 50% SOC. The battery performance is notational down below minus battery temperature owing to a poor chemical reaction even though in the different battery alloy structure.
- (4) Both battery types slightly decrease the AC impedance in the high battery temperature (50 degrees C) to the standard (22 degrees C). The variation level is small by comparison with the low battery temperature to the standard.

#### Acknowledgments

This study is partly sponsored the Japan Society for Promotion of Science (JSPS) under Grants-in-Aid for Scientific Research (No.24560273; Optimum group control technology for on-board energy storage devices of EVs and HEVs).

#### References

- 1) Kameyama, H.; *Study on Heat Generation Behavior at Small Lithium-ion Secondary Battery*, JSME No.02-7 The 8<sup>th</sup> Symposium on Prime Mover and Energy Engineering, Tokyo, (2002), pp.387-392 (in Japanese).
- 2) Mueller, J. M.; *Characterization of Direct Methanol Fuel Cells by AC Impedance Spectroscopy*, Journal of Power Sources 75, (1998), pp.139-143.
- 3) Itagaki, M.; *Electrochemical Impedance Method*, Maruzen, Tokyo, (2011), pp.61-62 (in Japanese).
- 4) Konomi, T.; *Research on PEFC Overvoltage Analysis Method by Impedance Technique*, Transactions of the Japan Society of Mechanical Engineers, Series B, Vol.72, No.723 (2006), pp.192-197 (in Japanese).
- 5) Konomi, T.; *Research on Diagnosis Technique on PEFC Running Condition*, Transactions of the Japan Society of Mechanical Engineers, Series B, Vol.71, No.701 (2005), pp.245-250 (in Japanese).
- 6) Tachibana, K.; *Impedance Measurement Know-how and Data Analysis Method*, Technical Information Association, Tokyo, (2012), pp.57-66 (in Japanese).